# CFD Modeling of Air Flow on Wall Deposition in Different Spray Dryer Geometries

**Article** *in* Drying Technology · February 2015

Impact Factor: 1.52 · DOI: 10.1080/07373937.2014.966201



**4 authors**, including:

Samaneh Keshani
National University of Malaysia, (UKM)
**12** PUBLICATIONS **93** CITATIONS
SEE PROFILE

Mohammad Hossein Montazeri
Shiraz University
**1** PUBLICATION **3** CITATIONS
SEE PROFILE

Wan Ramli Wan Daud
National University of Malaysia
**420** PUBLICATIONS **4,620** CITATIONS
SEE PROFILE



Drying Technology: An International Journal
Publication details, including instructions for authors and subscription information:
http://www.tandfonline.com/loi/ldrt20

# CFD Modeling of Air Flow on Wall Deposition in Different Spray Dryer Geometries

Samaneh Keshani[ab], Mohammad Hossein Montazeri[c], Wan Ramli Wan Daud[ad] & M. Mohsen Nourouzi[be]

[a] Institute of Fuel Cell Technology, University Kebangsaan Malaysia, Bangi, Malaysia

[b] Institute of Tropical Forestry and Forest Products, University Putra Malaysia, Selangor, Malaysia

[c] Department of Mechanical Engineering, Shiraz University, Shiraz, Iran

[d] Department of Chemical and Process Engineering, Faculty of Engineering, University Kebangsaan Malaysia, Bangi, Malaysia

[e] Islamic Azad University Isfahan, Khorasgan Branch, Isfahan, Iran

Accepted author version posted online: 02 Feb 2015.Published online: 02 Feb 2015.

To cite this article: Samaneh Keshani, Mohammad Hossein Montazeri, Wan Ramli Wan Daud & M. Mohsen Nourouzi (2015): CFD Modeling of Air Flow on Wall Deposition in Different Spray Dryer Geometries, Drying Technology: An International Journal, DOI: 10.1080/07373937.2014.966201

To link to this article: http://dx.doi.org/10.1080/07373937.2014.966201

*Drying Technology*, 0: 1–12, 2015

ISSN: 0737-3937 print/1532-2300 online
DOI: 10.1080/07373937.2014.966201

Taylor & Francis
Taylor & Francis Group

# CFD Modeling of Air Flow on Wall Deposition in Different Spray Dryer Geometries

**Samaneh Keshani,[1,2] Mohammad Hossein Montazeri,[3] Wan Ramli Wan Daud,[1,4] and M. Mohsen Nourouzi[2,5]**

[1]*Institute of Fuel Cell Technology, University Kebangsaan Malaysia, Bangi, Malaysia*
[2]*Institute of Tropical Forestry and Forest Products, University Putra Malaysia, Selangor, Malaysia*
[3]*Department of Mechanical Engineering, Shiraz University, Shiraz, Iran*
[4]*Department of Chemical and Process Engineering, Faculty of Engineering, University Kebangsaan Malaysia, Bangi, Malaysia*
[5]*Islamic Azad University Isfahan, Khorasgan Branch, Isfahan, Iran*



**Wall deposition is one of the most conventional problems in the spray drying process. The operation of a spray dryer is affected by the wall deposition fluxes inside the equipment. In this study, computational fluid dynamic (CFD) simulation was used to investigate the effect of spray dryer geometry on wall deposition. A CFD model was developed for different geometries of spray dryer with a conical (case A) or a parabolic (cases B and C) bottom. The results implied that the parabolic geometry resulted in a lower deposition rate on the spray dryer walls. A comparison of results using the P-values (F-test) of the air velocity, in the conical and parabolic geometries, showed that there was a significant difference in air stability between them. The flow field in conical geometry case A was significantly more unstable, and parabolic geometry case C produced the most uniform airflow patterns. Moreover, the higher wall shear stress in case C, with lower values of the vorticity, would result in less wall deposition.**

**Keywords** Air flow; Computational fluid dynamics (CFD); Cone geometry; Parabolic geometry; Spray dryer; Vortex; Vorticity; Wall deposition; Wall shear stress

## INTRODUCTION

Spray drying is the transformation of feedstock from a fluid state into a dried particle form, by spraying the feed into a hot drying medium.[1] The feed can either be in solution, suspension, emulsion, or paste form. The properties of the dried product depend on the physical and chemical characteristics of the feed, as well as the dryer design and operation. Normally, spray dryers are installed at the end of the process, and it is an important step at which the quality of the final powder is controlled. Particle sticking on the wall surfaces occurs throughout the spray drying process. The deposition is observed on the walls inside the drying chamber, the exhaust system, cyclones, and the packing lines.[2] However, the wall deposition is generally attributed to powder around the cylindrical and conical chamber walls.[3] The deposition is not desirable, as oxidized particles give a brownish hue to final products, which lowers the quality and safety. Combustion of the organic powder deposits may cause fires and explosions in spray dryers. Wall deposition affects product yield, as it sticks to the spray dryer and causes excessive plant downtime, as the dryer must be stopped to allow removal.[4] The degree of wall deposition is affected by several factors, including operating parameters such as airflow patterns (chamber geometry and position of inlet–outlet port), primary conditions (inlet temperature, air flow rate, flow rate of liquid feed, and particle size), and wall properties (wall materials).[5] One of the primary factors that influences the quality of the products produced by a spray dryer is the chamber geometry. This directly influences the airflow pattern, and consequently the behavior and flow pattern of particles within the dryer.[6] The significance of wall deposition and its complex mechanisms have resulted in considerable research, either experimental or theoretical. In parallel with the experimental studies on the spray drying process, computational fluid dynamics (CFD) simulation has also been widely used to simulate and analyze fluid dynamic behaviors in a spray dryer.[7] This technique generally involves predicting the internal flow field of a spray dryer chamber, from which the injected droplets are tracked to see how the spray dryer performs.[5]

A two-dimensional axisymmetric transient model simulation of droplet–droplet interactions, displacing the region of heat and mass transfer from the central core toward the periphery of the drying chamber, has been published by Mezhericher et al.[8] Their study also noted that insulation of the spray dryer can substantially affect temperature and

Correspondence: Samaneh Keshani, Institute of Fuel Cell Technology, University Kebangsaan Malaysia, 43600 UKM Bangi, Malaysia; E-mail: sa.keshani@yahoo.com

Color versions of one or more of the figures in the article can be found online at www.tandfonline.com/ldrt.

humidity patterns, whereas its influence on the velocity flow field is less marked.

Research by Johansson et al.[9] and Westerberg et al.[10] describes the design of the first numerical approach toward resolving the flow dynamics in the regeneration reactor, together with the temperature and particle distribution.[11] The study by Johansson et al.[11] carried out a CFD numerical simulation of the dynamics of a second-order spray roasting process, and a two-way coupled Eulerian–Lagrangian approach. The CFD simulation was used to investigate the influence of a changed spray nozzle position on the flow characteristics of the continuous and dispersed phase, and the relationship between temperature and energy efficiency and the regeneration process. The energy balances in the process, with evaporation of droplets and heat loss through walls, were described.

Simulation of the transient flow behavior in a pilot scale spray dryer was presented by Langrish et al.[12] They reported the modeling showed significant differences across the no swirl cases, where a central air jet was seen to wobble with a large-scale eddying motion outside the dryer axis, because of the strong precession of the central air jet at moderate swirl to vortex breakdown, and with reverse flow occurring on the axis of the dryer at high swirl.

Huang et al.[13] carried out a CFD simulation of the evaporation of droplets. In their study, three polynomial functions for the falling rate period, based on the concept of characteristic drying rate, were proposed and examined.

Jamaleddine and Ray[14] studied the drying of sludge in a cyclone dryer using CFD. They added a user-defined subroutine to extend the ANSYS FLUENT capabilities to account for properties, and to simulate the constant and falling rate drying periods.

Zhou et al.[15] used a CFD simulation of a sudden expansion, mimicking a spray dryer. In their study, the reported low inlet velocity resulted in a more uniform deposition pattern. The contrasting deposition behavior is attributed to the combined effect of the integral time scale, relative fluctuation, and near-wall shear stress.

Harvie et al.[4] used a tall form spray dryer to evaluate the applicability of current CFD models of this type of simulation, and the characteristics of the flows that exist within these complex devices. They found that the simulated product moisture content was of the same magnitude, but generally slightly lower than that found during experiments. It was also found that the behavior of the dryer is largely determined by the relationship between the initial momentum of the injected particles and the gas flow field within the dryer.

Sadripour et al.[16] developed a CFD simulation of a spray dryer based on mathematical modeling and experimental trials in order to estimate and measure the wall deposition. In the modeling part of their study, they attempted to determine the effect of the particle diameter on the percentage of wall deposition and the position where it occurred. The model results obtained for wall deposition were then compared with collected experimental data, and good agreement was observed.

The indirect techniques using fluid flow to remove particles are very interesting, because they mimic hydrodynamic conditions that exist in the process of the removal of surface deposits.[17] The wall shear stress has an important role in the removal of deposition, especially related to the determination of the parameters that allow an accurate prediction of the process in the equipment.[17,18] The wall shear stress required to remove a particle from a solid substrate can be estimated by different model systems, such as parallel plate flow cell, where the flow runs parallel to the solid surface[19]; impinging jets[20]; or radial flow cell.[21,22] The wall shear stress should be independent of the flow rate, for a given particle and substance.[21,23,24]

The first analytical and empirical models to compute the wall shear stress for both laminar and turbulent ideal diverging flows between two parallel discs were developed by Moller.[25] Kota and Langrish[26] estimated wall shear stress for the conical section of the spray dryer at three locations by various methods, depending on the geometry and flow conditions.

The work of Zhou et al.[15] studied a sudden pipe expansion that mimicked a spray dryer. Varying the inlet Reynolds number by changing the inlet air velocity resulted in contrasting deposition patterns. They used a CFD validation model to elucidate this phenomenon. The contrasting deposition behavior was attributed to the combination of the effect of the integral time scale, relative fluctuation, and near-wall shear stress.

Cylinder-on-cone or simple cylindrical chamber geometries are currently the most popular spray dryer chamber geometries. The aim of this study is to develop a CFD model to predict the effect on wall deposition of three types of spray dryer geometry and airflow pattern, and wall shear stress. This article is concerned with the analysis and design of supersonic gas flows in jet pumps.

## CFD BACKGROUND THEORIES

Numerical simulations have been done using the three-dimensional (3D) pressure-based solvers incorporated in ANSYS FLUENT. Both heat and momentum equations have been solved along with continuity equation (pressure correction equation in SIMPLE algorithm) with the aid of finite volume discretization. Regarding the high-speed flow and turbulent nature of flowfield, the RNG k–$\epsilon$ turbulent flow model was used because it yielded adequate accuracy at reasonable computer time, especially for swirling flows.[13] It has also been successfully used in previous modeling and simulations of spray dryers.[13,16,27] Theoretical equations that have been proposed in this investigation

are based on continuity–momentum–energy balances. These equations can be written in the following forms.

### Continuity Equation

The general form of the mass conservation equation which can be showed by

$$\frac{\partial \rho}{\partial t} + \frac{\partial(\rho u_i)}{\partial x_i} = M_m \tag{1}$$

for incompressible flows, where $\rho$ is the gas density, $u_i$ is the gas velocity vector components, and $M_m$ is the mass added to the system and any user-defined sources.

### Momentum Equation

Newton's second law of motion is written by

$$\frac{\partial(\rho u_i)}{\partial t} + \frac{\partial(\rho u_i u_j)}{\partial x_j} = -\frac{\partial P}{\partial x_i} + \frac{\partial}{\partial x_i}\left[\mu\left(\frac{\partial u_i}{\partial x_i} + \frac{\partial u_j}{\partial x_i}\right) - \overline{\rho u_i' u_j'}\right] + \rho g_i + M_F \tag{2}$$

where $P$ is the pressure of the fluid, $\mu$ is the viscosity, $\overline{\rho u_i' u_j'}$ is the turbulent shear stress, $g_i$ is gravitational acceleration, and $M_F$ is any momentum source term.

The turbulent kinetic energy $k$ and its dissipation rate $\epsilon$ for RNG $k-\varepsilon$ turbulence model are written by

$$\frac{\partial(\rho k)}{\partial t} + \frac{\partial(\rho k u_i)}{\partial x_i} = \frac{\partial}{\partial x_i}\left[\alpha_k \mu_{eff} \frac{\partial k}{\partial x_j}\right] + G_k + G_\varepsilon - \rho\varepsilon - Y_M + S_k \tag{4}$$

and

$$\frac{\partial(\rho\varepsilon)}{\rho t} + \frac{\partial(\rho\varepsilon u_i)}{\partial x_i} = \frac{\partial}{\partial x_j}\left[\alpha_\varepsilon \mu_{eff} \frac{\partial \varepsilon}{\partial x_j}\right] + C_{1\varepsilon}\frac{\varepsilon}{k}(G_k + C_{3\varepsilon}G_\varepsilon) - C_{2\varepsilon}\rho\frac{\varepsilon^2}{k} + S_\varepsilon \tag{5}$$

The turbulence viscosity can be obtained from Eq. (7):

$$\mu_{eff} = \mu + \mu_t \tag{6}$$

$$\mu_t = \rho C_\mu \frac{k^2}{\varepsilon} \tag{7}$$

The model constants values are set as: $C_{1\varepsilon} = 1.4$, $C_{2\varepsilon} = 1.68$, $C_\mu = 0.0845$, $\alpha_k = \alpha_\varepsilon = 1.39$,[28] and $S_k$ and $S_\varepsilon$ are user-defined source terms. The terms $G_k$ and $G_\varepsilon$ are, respectively, the predictions of the turbulence kinetic energy due to the mean velocity gradients and the buoyancy.

The value of wall shear stress in turbulent boundary layers is obtained from the from the following equations

$$V/V_\tau = 2.5\, ln(V_\tau y/v) + 5.45 \tag{8}$$

$$V_\tau = \sqrt{\frac{\tau_w}{\rho}} \tag{9}$$

where $y$ is the normal distance from the wall, $V_\tau$ is the magnitude of the friction velocity, $v$ is the kinematic viscosity, $V$ is the velocity of the fluid, and $\tau_w$ is the magnitude of the wall shear stress.

### Energy Equation

The energy balance can be written as

$$\frac{\partial(\rho c_p T)}{\partial t} + \frac{\partial(\rho c_p u_i T)}{\partial x_i} = \frac{\partial}{\partial x_i}\left[k\frac{\partial T}{\partial x_i} - \overline{\rho u_i' T'}\right] + M_h \tag{3}$$

where $c_p$ is the specific heat capacity, $T$ is the temperature, $k$ is the thermal conductivity, is the work done by turbulency, and $M_h$ is any source term.

## CHAMBER DESIGN AND BOUNDARY CONDITIONS

A co-current spray dryer with a 24-vane centrifugal atomizer was used for this study. The three-dimensional geometry was constructed using ANSYS Design Modeler, and hexahedral meshes were used to provide more stability in the numerical solution. The hexahedral meshes are shown in Fig. 1.

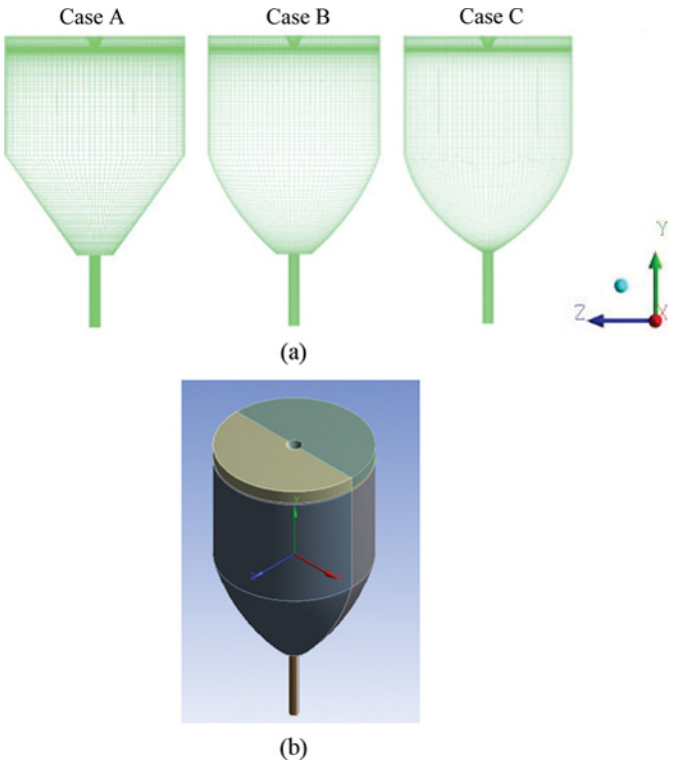


FIG. 1. (a) Computational meshes from the front of the domain at different geometries. (b) Place of origin coordinates.

TABLE 1
Size of geometries tested

| Case | Type of geometry | Number of elements | Minimum orthogonal | Maximum aspect ratio |
|---|---|---|---|---|
| **A** | Conical | 1223675 | $7.41 \times 10^{1}$ | $5.49 \times 10^{1}$ |
| **B** | Parabolic 1 | 1223675 | $6.90678 \times 10^{-1}$ | $5.49503 \times 10^{1}$ |
| **C** | Parabolic 2 | 1219525 | $5.14365 \times 10^{-1}$ | $4.94026 \times 10^{1}$ |

A summary of the boundary is presented in Table 1. At the inlet, the velocity of drying air was 8.09 m/sec, without and with spray. The temperature of the air at the inlet was set at 413 K, with corresponding 80% relative humidity. The air inlet mass flow rate can be computed to be 70.2 kg/hr. The outlet vacuum gauge pressure was measured experimentally at room temperature by a U-tube manometer without heating. The determined vacuum pressure was taken as the basis for all simulations, and was assumed to be a good approximation for all inlet conditions considered (it is assumed that the inlet condition cannot change the outlet pressure considerably). The outlet pressure was set at −372.4 Pa. The value of the convective heat transfer coefficient, 95 ($Wm^{-2}K^{-1}$), was determined by trial and error in order to match the inlet and outlet temperatures of the dryer operation without spray. An experimental investigation showed that a dry run at dryer unit inlet temperature of 140°C without atomizer rotation exhibited an outlet temperature of 103°C with chamber walls 2 cm stainless steel. The turbulence kinetic energy and dissipation rate gave an estimate of the inlet air Reynolds number and the opening size (FLUENT Manual 14.0). Case A has a cylinder-on-cone chamber geometry, and cases B and C have parabolic chamber geometries. The methods to obtain the boundary and initial conditions are presented in Table 2. The 3D CFD numerical simulations for the three spray dryer geometries are shown in Fig. 1. In case A, the bottom of the chamber has a 60° cone angle. In cases B and C, the bottom of the chamber is parabolic with functions and the origin coordinates as follows

Case B:

$$y = 0.03x^2 + 0.295x - 59.865 \tag{10}$$

Case C:

$$y = 0.0347x^2 + 0.0051x - 55.655 \tag{11}$$

TABLE 2
Boundary and initial conditions

| Properties | Value |
|---|---|
| **Inlet:** | |
| Inlet air temperature (°C): | 140 |
| Velocity Inlet $\left(\frac{m}{s}\right)$ | 8.09 |
| Mass flow rate (kg/h) | 70.2 |
| Turbulent kinetic energy ($m^2/s^2$) | 0.265 |
| Turbulent dissipation rate ($m^2/s^3$) | 1.120 |
| Turbulence intensity (%) | 5 |
| Turbulent diameter (cm) | 2 |
| **Outlet:** | |
| Outlet vacuum gauge pressure (pa) | –372.4 |
| Outlet air temperature (°C) | 103 |
| **Wall:** | |
| Convective heat transfer coeff. ($W/m^2K$) | 95 |
| Free stream temperature (°C) | 27 |
| Material | Stainless steel |
| Thickness (cm) | 0.2 |
| Atomizer rotation (rad/s) | 1888 |

## RESULTS

### Time-Dependent Nature of the Flow

The general flow patterns were simulated at successive time steps in the spray dryer. The typical instantaneous velocity contours are displayed at different flow times in Fig. 2 to indicate the time-dependent nature of the flow patterns. The use of time-dependent simulation proved essential, due to the prediction of transient flow behavior that had been experimentally tested. Comparison of the velocity profiles shows that the simulated flow field is dependent on the simulated time. The velocity is a function of time and indicates the time-dependent nature of the flow patterns, which is consistent with the findings of Langrish et al. and Woo et al.[12,27] Considerable change in the velocity contours shows the importance of time-dependent simulation of flow behavior. The present observations are in agreement with the theory put forward by Langrish et al.[12] Figure 3 represents the velocity–time graphs of the three cases at multiple points. It was observed that the velocity is time-dependent and variable. However, the velocities of cases A and B have larger amplitude compared to case C. The velocities of cases A, B, and C, show that the simulations are successful in predicting the processing airflow patterns. An unstable precession motion is exhibited in cases A and B, while a stronger and more coherent precession motion is observed in case C.

### Effect of Spray Dryer Chamber Geometry, Airflow, and Wall Shear Stress on Wall Deposition

Cylinder-on-cone or simple cylindrical chamber geometrics are currently the most popular ones in spray dryers. Several researchers have studied other possible chamber formations than pure conical, such as lantern, hour-glass geometries,[6,29] and horizontal configurations.[30] It should be noted that the cylinder geometry can impact drying

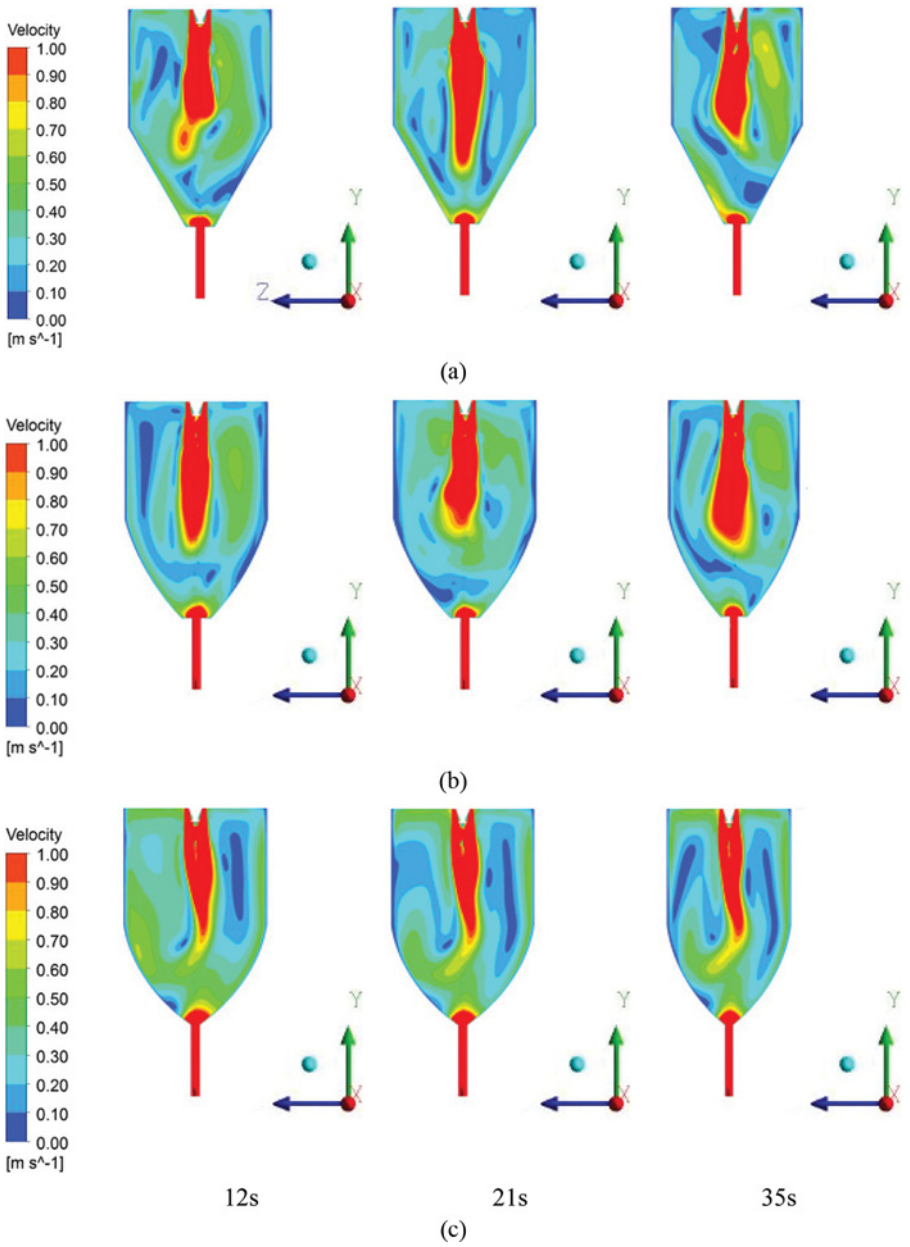


FIG. 2. Velocity contour plots of the spray dryer at different times at transient condition: (a) case A, (b) case B, and (c) case C.

performance. Another possible parameter for the drying chamber may be the parabolic configuration.

The drying process will be affected significantly by the airflow patterns. Understanding the features of the airflow inside a spray dryer is essential to the investigation of the resulting complicated droplet trajectories and wall deposition.[12] The effect of flow patterns on wall deposition in a spray dryer was studied by Southwell and colleagues.[31,32] They observed an unstable time-dependent air flow. It was characterized by random switching of flows in significant portions between clockwise, anti-clockwise, and chaotic turbulent flow regimes. Such an uncontrolled situation would probably result in undesirable amounts of wall deposition.

The strongest low-frequency oscillations were predicted by the CFD program used by Oakley and Bahu,[33] where runs were in time-dependent mode. In their study, it is shown that conditions with sufficient swirl in the inlet air cause a vortex breakdown, a central recirculation zone, and a processing vortex core. The successful prediction of vortex breakdown is an important step in assessing the effect of a processing vortex core on wall deposition, and of a central recirculation zone on overheating and overdrying

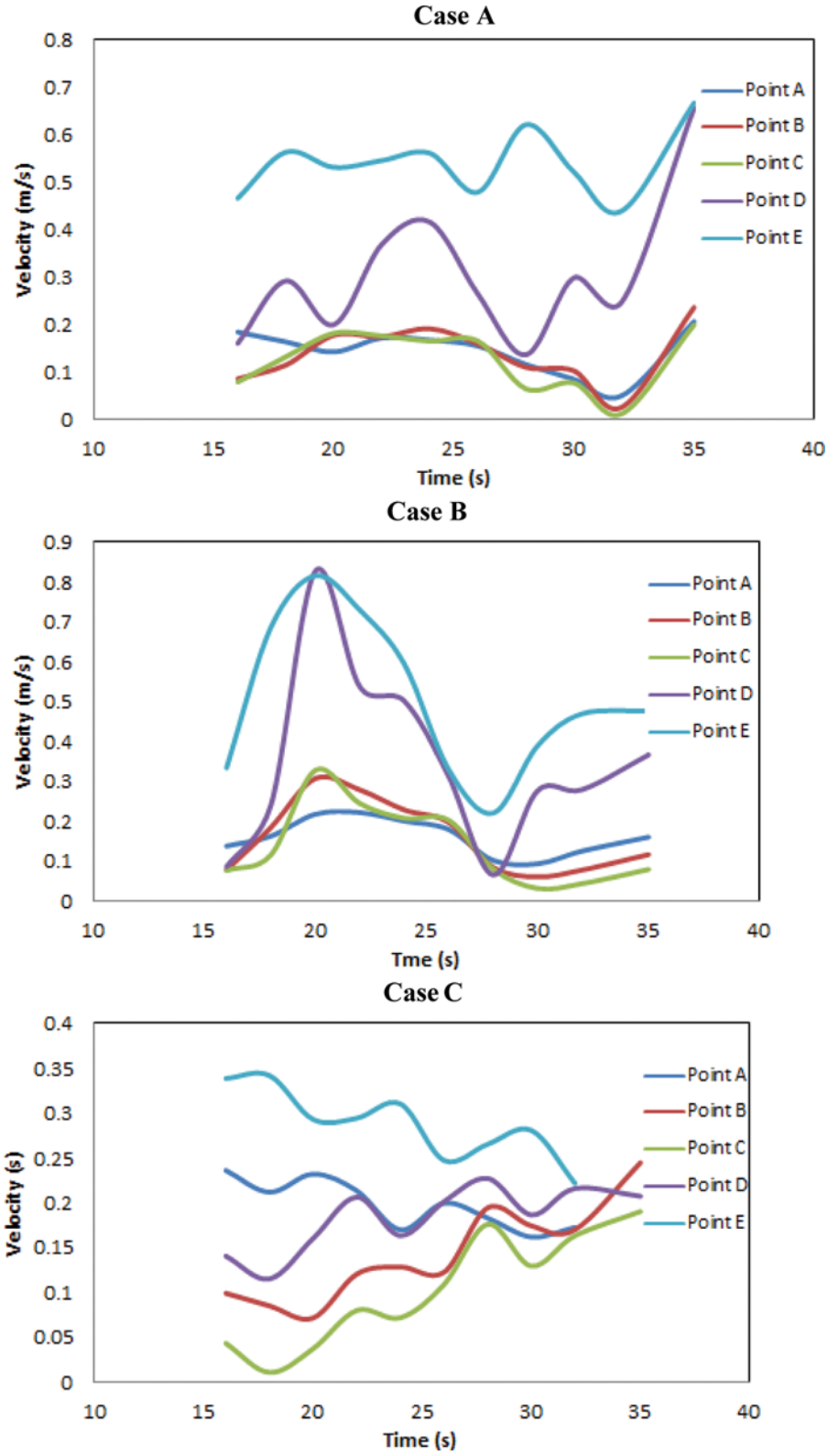


FIG. 3. Velocity plots of the spray dryer at periodic times at transient condition.

of particulate material, as small and medium-sized particles tend to be entrained in recirculation zones.

Chen et al.[34] suggested a combination of modified near-wall airflow patterns, and inlet temperature distribution could be used to significantly reduce wall deposition in industrial-scale spray drying of milk in New Zealand. Although they were unable to reach quantitative conclusions about the effect of dryer operating parameters, such changes are likely to be substantially less costly than making major modifications to the design of an existing dryer. The history of ideas and designs proposed for the reduction of wall deposition has been reviewed by Masters,[35] who concluded that CFD techniques offered assistance in finding practical solutions.

In the present study, the air entered from the center of the chamber and was directed straight downward. The flow pattern shows a high-velocity core flow zone with a circulation that is extended through the chamber. A two-sample F-test, with a cut-off of $p < 0.05$ for inequality, was used to analyze air flow stability inside the drying chamber. The average velocity for the three drying cylinder geometries was measured at five varying levels: $y = 0.5$, 0.3, 0.0 (reference level), $-0.3$, and $-0.5$ m, as shown later in Fig. 6. It is observed from Table 3 that the P-values of the velocity of air for cases A–C and B–C are $<0.05$, which shows that the flow fields in cases A and B are significantly more unstable than the flow field in case C. It seems that cases A and B are not significantly different. The stability of the flow patterns inside spray dryers affects the wall deposition.[12] It was observed that C is more stable than cases A and B. Case C also produced a more uniform airflow pattern, as shown in Fig. 2.

Higher velocity increases the chance of wall deposition, due to the higher collision velocity of droplets against the wall. On the other hand, Xu et al.[36] studied the velocity pattern inside the chamber. They found that higher velocities yielded higher wall collision and higher erosion of the internal wall; higher velocity also gives a larger relative fluctuation, causing more particles to be dispersed to the wall and, at the same time, the greater shear stress from the higher inlet velocity, which results in the reduction of wall deposition.[15] The average velocities for the conical and parabolic geometrics of the three spray dryers are shown in Table 4. The placements of the points on the walls are shown in Fig. 4. It was observed that the flow field at points in case C are greater than those in cases A and B.

TABLE 4
Average velocity of points for Cases A, B, and C

| Point | Point 1 | Point 2 | Point 3 | Point 4 | Point 5 |
|---|---|---|---|---|---|
| Case A | 0.1709 | 0.1495 | 0.1271 | 0.2512 | 0.4442 |
| Case B | 0.2362 | 0.2611 | 0.2392 | 0.3286 | 0.6198 |
| Case C | 0.2942 | 0.3526 | 0.2959 | 0.3834 | 0.6419 |

Figure 4 shows that wall shear stress obtained in A increases toward the bottom of the conical section. Therefore, this suggests that in high-velocity conditions, the shear stress might play an important role in particle removal. This effect seems to outweigh the effect of particle dispersion. In case C, the velocity of air near the junction of the vertical and conical walls has the highest value, compared to cases A and B. The higher velocity of airflow around the walls decreases wall deposition of particles, due to larger shear stress. The average wall shear stress in cases A, B, and C is 0.0295, 0.0299, and 0.0348 Pa, respectively. The average wall shear stress for cases A and B is almost the same, due to their similar geometries.

The particle depositing at the wall can re-enter into the flow, which makes the deposition phenomenon even more complicated. Cleaver and Yates[37] studied particle removal on observed deposition rates. They showed that wall shear stress is a controlling parameter on particle re-entrainment and particle removal, due to turbulence bursts at the wall. The deposition varies linearly with time because it is below a critical value where removal can occur. If it is above the critical value, the deposited particles can re-enter the dryer.[38]

An integral part of fluid dynamics is vorticity. Vorticity and its study have been extremely important topics in almost all fluid dynamics courses in the past century and, as already noted, is considered to be a key ingredient of a turbulent flow. Vorticity is a crucial property of the flow, and problems associated with it relate mostly to its strength and location. In fluid dynamics, a vortex is a region within a fluid where the flow is mostly a rotating motion, around an imaginary axis or a common straight or curved center. That motion pattern is called a vertical flow. The swirling feature in flow fields is commonly referred to as a vortex. By most accounts,[39,40] a vortex is characterized by the swirling motion of fluid around a central region.[41] In most spray

TABLE 3
P-values of F-test for Cases A and C

| Level | Y = 0.5 | Y = 0.3 | Y = 0.0 | Y = −0.3 | Y = − 0.5 |
|---|---|---|---|---|---|
| P-value Case AC | 6.27734e-06 | 2.23352e-15 | 8.72553e-07 | 4.1346e-09 | 9.75317e-13 |
| P-value Case BC | 0.004824096 | 5.89883e-13 | 3.26074e-06 | 2.76751e-8 | 5.25205e-15 |

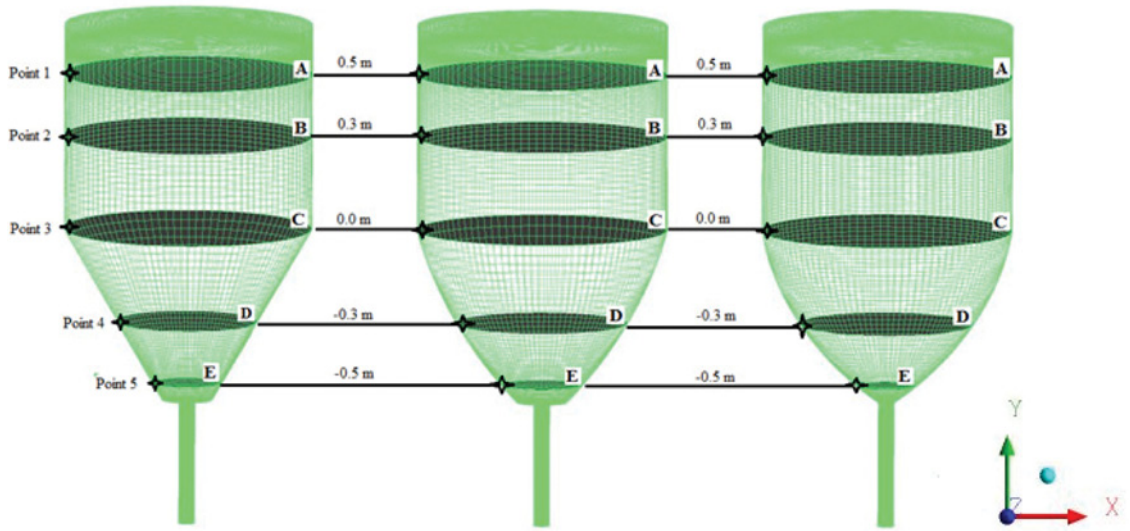


FIG. 4. Schematic diagrams of the three different types of drying chamber geometries at various levels and points.



dryers, the air entering the inlet with a tangential velocity component is a vortex. The rotation of the atomizer causes the strong vortex to move closer to the walls, and for particles to be deposited there.[12] The air vorticity in cases A and B is higher than in case C, as presented in Table 5. In addition, Fig. 5 shows that the air vortex in cases A and B is closer to the walls compared to case C. According to the results obtained from the CFD simulation, it is predicted that the parabolic geometry of case C produces less wall deposition. Hence, it could be used to reduce wall deposition problems.

## CFD Qualitative Trend Validation

In this study, the level of accuracy in the prediction of the parameters is determined via CFD qualitative trend validation. A well-known fact in modeling of spray dryers is that validation is very difficult. Wall shear stress is a determining factor in the removal of particle deposition during the spray drying process. The ability to predict the wall shear stress is one aspect in CFD simulations. The correlation between the measured wall deposition flux rate inside the spray dryer and the simulated wall shear stress has been used as the key validation. The result of the CFD validation for case A assumptions is shown in Figs. 6 and 7. The CFD-predicted wall shear stress in the axial direction at different plates (top, middle, and bottom) is detailed in Fig. 6. It is suggested that the deposition flux rate will decrease with increasing distance from the atomizer, due to the increase in wall shear stress. Figure 7a demonstrates the experimental deposition flux rate versus wall shear stress at the different plates for skimmed milk, whey protein, full cream milk, and lactose, obtained by Keshani et al.[42,43] Due to the rotary atomizer, the top plate exhibits a higher deposition flux rate compared to the middle and bottom plates, and relatively large and wet particles directly impinge the walls as they traverse the initial downward hot air flow. The wall shear stress is also lower than at the middle and bottom plates. Wall deposition at the middle plate mainly arises from left over particles moving downwards, which did not collide with the top plate, or were recirculated particles from the conical region of the chamber.[43] At the middle plate, wall deposition flux decreases due to the high wall shear stress. The wall shear stress is greater at the bottom plate, while the deposition flux rate is low compared to the top plate, but greater than at the middle plate. The higher deposition rate conflicts with the Cleaver and Yates[37] theory. This contradiction is attributed to the fact that the bottom plate is located on the inclined conical wall, and particles are affected by gravity settling. Therefore, it is concluded that the effect of the higher shear stress at the bottom plate is compensated by the effect of gravity settling. In addition, Fig. 7b shows the wall deposition of full cream milk at the three plates, where there is more deposition at the bottom plate than at the middle plate.

However, the phenomenon is even more complicated. Cleaver and Yates[37] studied particle removal on observed deposition rates and found that wall shear stress is a

TABLE 5
Area average of vortices for Cases A, B, and C

| Level | Y = 0.5 | Y = 0.3 | Y = 0.0 | Y = −0.3 | Y = −0.5 |
|---|---|---|---|---|---|
| Case A | 10.105 | 7.2392 | 6.6274 | 5.7547 | 18.4532 |
| Case B | 10.4669 | 7.0028 | 6.1457 | 4.7593 | 14.6559 |
| Case C | 9.0713 | 6.5000 | 5.6826 | 3.9249 | 28.0904 |

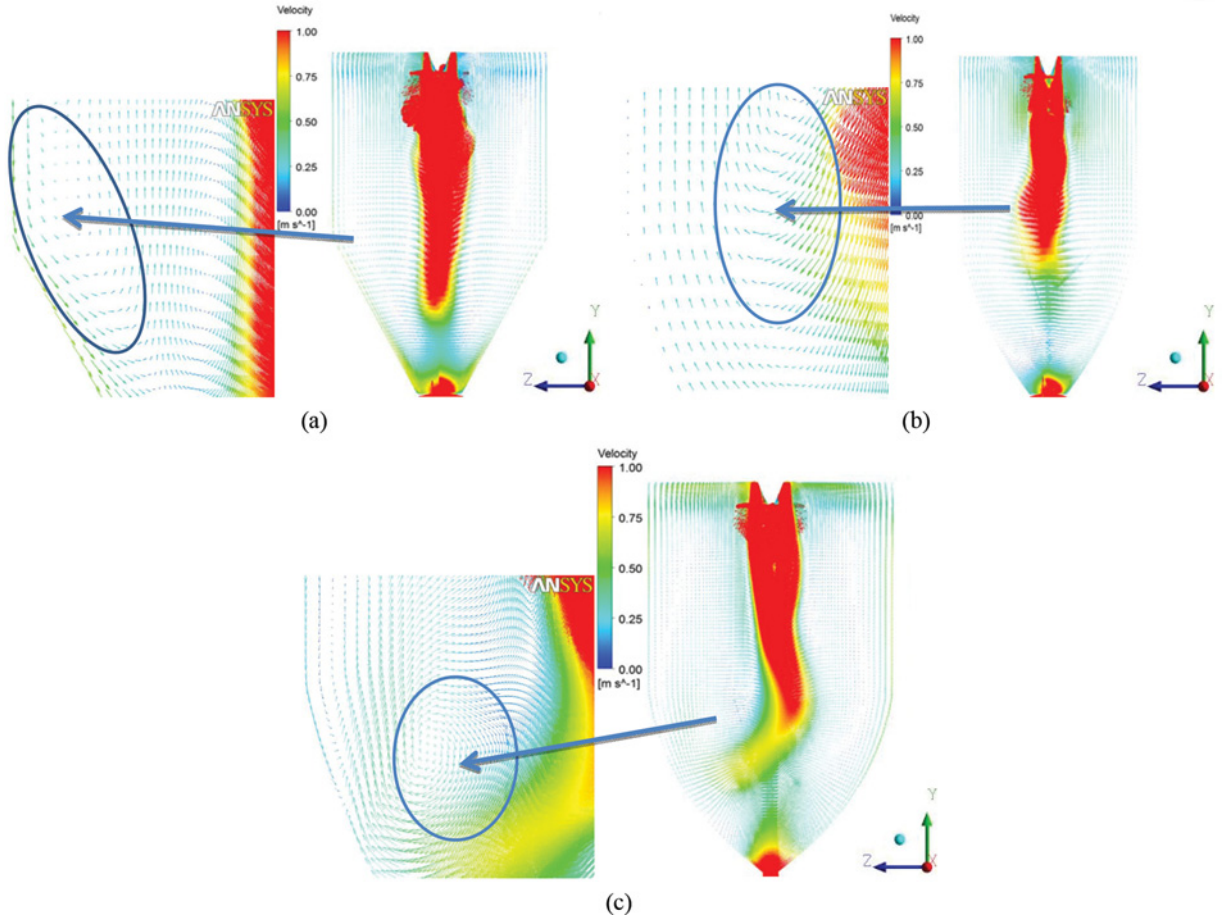


FIG. 5. Vectors velocity air flow patterns at transient condition at three cases: (a) case A, (b) case B, and (c) case C.

controlling parameter on particle re-entrainment. Figure 8 shows that deposition varies linearly with time, and because it is below a critical value, the deposited particles can re-enter the dryer. It was argued by Cleaver and Yates[37] that by remaining, the deposition particle mass per unit surface can be approximately computed. Figure 8 shows the relationship between $M(t_d, t)/M_0(t_d)$ and the magnitude of the friction velocity $|V_\tau|$. The re-entrainment or removal rate occurs if $V_\tau$ is higher than the critical value $V_{cr}$. A skip of $M(t_d, t)/M_0(t_d)$ can be observed at $V_{cr}$. The model by Cleaver and Yates[37] indicates that the deposit removal rate increases as the friction velocity or consequently the wall shear stress increases.

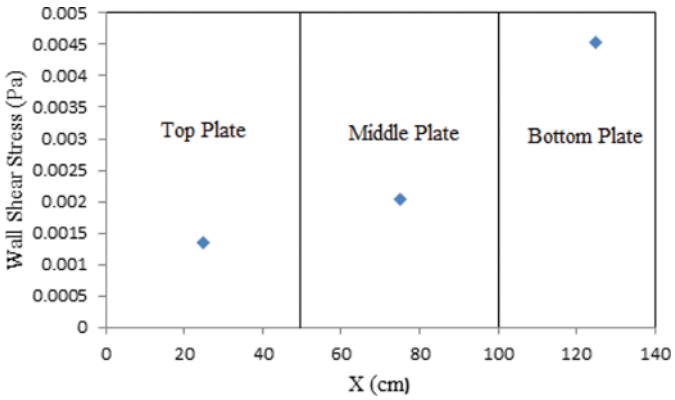


FIG. 6. Predicted wall shear stress in the axial direction at different plate.

## SUMMARY AND CONCLUSIONS

In this article, modeling the effect of flow behavior on wall deposition in different spray dryer geometries has been proposed. The CFD model was developed for three geometrical shapes with either a conical or a parabolic bottom. The velocity values over time showed a time-dependent nature of the flow in the spray dryer. The analysis of variance (ANOVA) test of velocity values in different spray dryer geometries showed that the parabolic bottom design can produce a more uniform airflow pattern, compared to the conical bottom. The results also showed that velocity had positive and negative effects on the deposition rate on the spray dryer walls. However, the greater shear stress due to the higher air velocity outweighed the effect of particle collision, and caused a reduction in the deposition rate. In

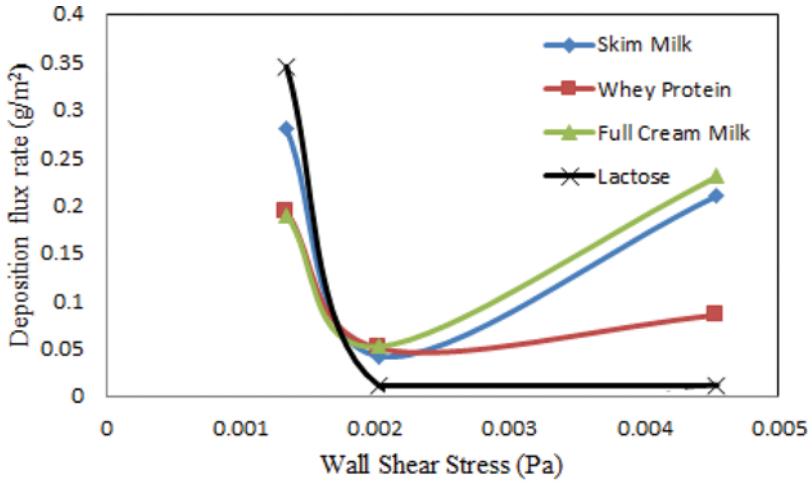


(a)

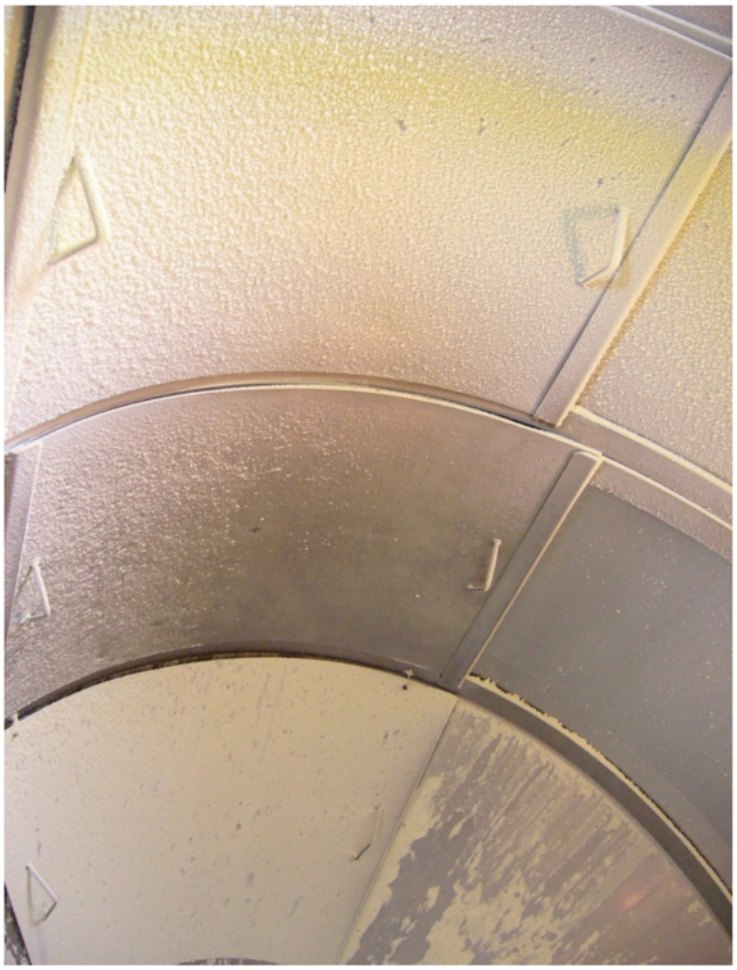

(b)

FIG. 7. (a) Comparison of the experimental deposition flux rate among predicted wall shear stress for different types of materials. (b) Wall depositions of full cream milk at three plates.

addition, higher values of vorticity in the conical bottom design boosted the deposition rate on the top and middle parts of the spray dryer. The results of CFD simulation suggest that the parabolic design of the bottom part of the spray dryer can enhance the drying performance by decreasing the deposition rate on the spray dryer walls.

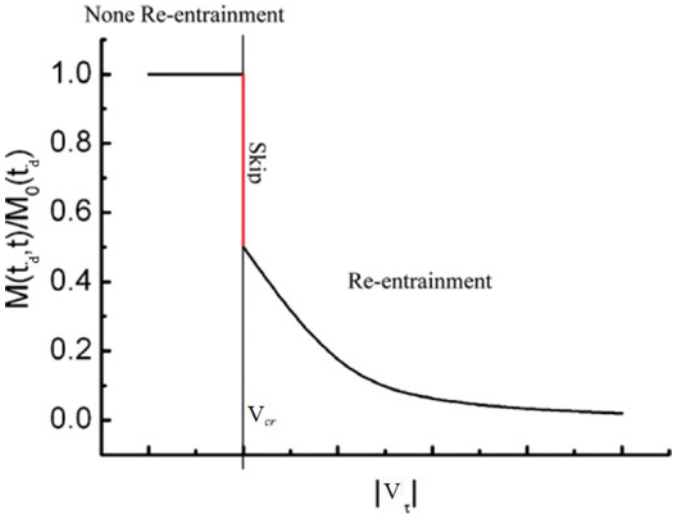


FIG. 8. The ratio of the remaining particle mass M($t_d$, $t$) and the deposit particle mass $M_0(t_d)$.[38]

## ACKNOWLEDGMENT

The authors greatly appreciate Dr. Meng Wai Woo at the Monash University, Australia, for sharing constructive ideas in CFD part for this study.

## FUNDING

The authors express their great appreciation to the Fuel Cell Institute, National University of Malaysia for its financial support to complete this research (UKM-GUP-2011-368 and DIP-2012-27).

## NOMENCLATURE

| | |
|---|---|
| $G_k$ | production of turbulence kinetic energy due to the mean velocity gradients |
| $G_\varepsilon$ | production of turbulence kinetic energy due to buoyancy |
| $M_m$ | source term in continuity equation |
| $M_F$ | source term in momentum equation |
| $M_h$ | source term in energy equation |
| $u_i$ | gas velocity vector (m/s) |
| $g_i$ | gravity component ($m^2/s$) |
| $S_k$ | user defined source term |
| $S_\varepsilon$ | user defined source term |
| $c_p$ | heat capacity (J/kg·K) |
| T | temperature (k) |
| t | time (s) |

### Greek Letters

| | |
|---|---|
| $\rho$ | density ($kg/m^3$) |
| $\mu$ | viscosity (kg/m.s) |
| $k$ | the turbulent kinetic energy ($m^2/s^2$) |
| $\varepsilon$ | energy dissipation rate ($m^2/s^3$) |
| $\mu_t$ | turbulent viscosity (kg/m.s) |
| $V_\tau$ | friction velocity (m/s) |
| $\tau_w$ | wall shear stress ($kg/ms^2$) |

## REFERENCES

1. Masters, K. *Spray Drying Handbook*, 3rd ed.; G. Godwin: New York, 1994.
2. Keshani, S.; Daud, W.R.W.; Woo, M.W.; Talib, M.Z.M.; Chuah, A.L.; Russly, A. Artificial neural network modeling of the deposition rate of lactose powder in spray dryers. *Drying Technology* **2012**, *30*(4), 386–397.
3. Chiawchanwattana, C.; Triratanasirichai, K. The effect of inlet temperature on the wall temperature behavior of salt powders produced by spray-drying. *Advanced Materials Research* **2012**, *550*, 704–708.
4. Harvie, D.J.E.; Langrish, T.A.G.; Fletcher, D.F. A computational fluid dynamics study of a tall-form spray dryer. *Food and Bioproducts Processing* **2002**, *80*(3), 163–175.
5. Woo, M.W.; Sadashiv, A.; Ramli, W. *Spray Drying: Operation, Deposition and CFD Modelling*. VDM Publishing: Saarbrücken, Germany, 2010.
6. Huang, L.; Kumar, K.; Mujumdar, A.S. Use of computational fluid dynamics to evaluate alternative spray dryer chamber configurations. *Drying Technology* **2003**, *21*(3), 385–412.
7. Keshani, S.; Daud, W.R.W.; Nourouzi, M.; Namvar, F.; Ghasemi, M. Spray drying: An overview on wall deposition, process and modelling. *Journal of Food Engineering* **2015**, *146*, 152–162.
8. Mezhericher, M.; Levy, A.; Borde, I. Droplet–droplet interactions in spray drying by using 2D computational fluid dynamics. *Drying Technology* **2008**, *26*(3), 265–282.
9. Johansson, S.; Geza, V.; Westerberg, L.; Jakovics, A. Characteristics of flow and temperature distribution in a Ruthner process. In *Proceedings of the International Scientific Colloquium: Modelling for Material Processing*. Riga, Latvia, September 16–17, 2010.
10. Westerberg, L.G.; Geza, V.; Jakovics, A.; Lundström, T.S. Burner backflow reduction in regeneration furnace. *Engineering Applications of Computational Fluid Mechanics* **2011**, *5*(3), 372–383.
11. Johansson, S.; Westerberg, L.G.; Lundström, T.S. Gas and particle flow in a spray roaster. *Journal of Applied Fluid Mechanics* **2014**, *7*(2), 187–196.
12. Langrish, T.; Williams, J.; Fletcher, D. Simulation of the effects of inlet swirl on gas flow patterns in a pilot-scale spray dryer. *Chemical Engineering Research and Design* **2004**, *82*(7), 821–833.
13. Huang, L.; Kumar, K.; Mujumdar, A.S. Simulation of a spray dryer fitted with a rotary disk atomizer using a three-dimensional computational fluid dynamic model. *Drying Technology* **2004**, *22*(6), 1489–1515.
14. Jamaleddine, T.J.; Ray, M.B. The drying of sludge in a cyclone dryer using computational fluid dynamics. *Drying Technology* **2011**, *29*(12), 1365–1377.
15. Zhou, Z.; Woo, M.; Clugston, R.; Chen, X. Deposition behavior in a sudden pipe expansion mimicking a spray dryer. Presented at CHEMECA 2011: Engineering a Better World, Sydney, NSW, Australia, September 18–21, 2011, 862.
16. Sadripour, M.; Rahimi, A.; Hatamipour, M.S. Experimental study and CFD modeling of wall deposition in a spray dryer. *Drying Technology* **2012**, *30*(6), 574–582.
17. Guillemot, G.L.; Vaca-Medina, G.; Martin-Yken, H.; Vernhet, A.; Schmitz, P.; Mercier Bonin, M. Shear-flow induced detachment of Saccharomyces cerevisiae from stainless steel: Influence of yeast and solid surface properties. *Colloids and Surfaces B: Biointerfaces* **2006**, *49*(2), 126–135.

18. Jensen, B.B.; Friis, A. Predicting the cleanability of mix-proof valves by use of wall shear stress. *Journal of Food Process Engineering* **2005**, *28*(2), 89–106.
19. Boonaert, C.J.; Dufrene, Y.F.; Rouxhet, P.G. Adhesion (primary) of microorganisms onto surfaces. In *Encyclopedia of Environmental Microbiology*; Bitton, G., Ed.; Wiley: New York, 2002.
20. Bundy, K.; Harris, L.; Rahn, B.; Richards, R. Measurement of fibroblast and bacterial detachment from biomaterials using jet impingement. *Cell Biology International* **2001**, *25*(4), 289–307.
21. Demilly, M.; Brechet, Y.; Bruckert, F.; Boulange, L. Kinetics of yeast detachment from controlled stainless steel surfaces. *Colloids and Surfaces B: Biointerfaces* **2006**, *51*(1), 71–79.
22. Detry, J.G.; Jensen, B.B.B.; Sindic, M.; Deroanne, C. Flow rate dependency of critical wall shear stress in a radial-flow cell. *Journal of Food Engineering* **2009**, *92*(1), 86–99.
23. Jensen, B.B.; Friis, A. Critical wall shear stress for the EHEDG test method. *Chemical Engineering and Processing: Process Intensification* **2004**, *43*(7), 831–840.
24. Perni, S.; Aldsworth, T.G.; Jordan, S.J.; Fernandes, I.; Barbosa, M.; Sol, M.; Tenreiro, R.P.; Chambel, L.; Zilhao, I.; Barata, B. The resistance to detachment of dairy strains of Listeria monocytogenes from stainless steel by shear stress is related to the fluid dynamic characteristics of the location of isolation. *International Journal of Food Microbiology* **2007**, *116*(3), 384–390.
25. Moller, P.S. Radial flow without swirl between parallel disks having both supersonic and subsonic regions. *Journal of Basic Engineering* **1966**, *88*, 147.
26. Kota, K.; Langrish, T. Prediction of wall deposition behaviour in a pilot-scale spray dryer using deposition correlations for pipe flows. *Journal of Zhejiang University Science A* **2007**, *8*(2), 301–312.
27. Woo, M.W.; Daud, W.R.W.; Mujumdar, A.S.; Wu, Z.; Talib, M.Z.M.; Tasirin, S.M. Non-swirling steady and transient flow simulations in short-form spray dryers. *Chemical Product and Process Modeling* **2009**, *4*(1).
28. Versteeg, H.K.; Malalasekera, W. *An Introduction to Computational Fluid Dynamics: The Finite Volume Method*, 2nd ed. Prentice Hall: Upper Saddle River, NJ, 2007.
29. Huang, L.; Kumar, K.; Mujumdar, A.S. A parametric study of the gas flow patterns and drying performance of co-current spray dryer: Results of a computational fluid dynamics study. *Drying Technology* **2003**, *21*(6), 957–978.
30. Huang, L.; Mujumdar, A.S. Numerical study of two-stage horizontal spray dryers using computational fluid dynamics. *Drying Technology* **2006**, *24*(6), 727–733.
31. Southwell, D.; Langrish, T. Observations of flow patterns in a spray dryer. *Drying Technology* **2000**, *18*(3), 661–685.
32. Southwell, D.B. Operability and performance assessment of spray dryers. Department of Chemical Engineering, Graduate School of Engineering, University of Sydney, 2000.
33. Oakley, D.; Bahu, R. Spray/gas mixing behaviour within spray dryers. In Drying'91, Amsterdam, 1991; 303–313.
34. Chen, X.; Lake, R.; Jebson, S. Study of milk powder deposition on a large industrial dryer. *Food and Bioproducts Processing* **1993**, *71*(3), 180–186.
35. Masters, K. Deposit-free spray drying: Dream or reality? In *Proceedings of the 10th International Drying Symposium (IDS '96), Drying*; Krakow, Poland, August 1996.
36. Xu, P.; Wu, Z.; Mujumdar, A.S.; Yu, B. Innovative hydrocyclone inlet designs to reduce erosion-induced wear in mineral dewatering processes. *Drying Technology* **2009**, *27*(2), 201–211.
37. Cleaver, J.; Yates, B. The effect of re-entrainment on particle deposition. *Chemical Engineering Science* **1976**, *31*(2), 147–151.
38. Jin, Y.; Chen, X.D. A fundamental model of particle deposition incorporated in CFD simulations of an industrial milk spray dryer. *Drying Technology* **2010**, *28*(8), 960–971.
39. Lugt, H.J. *Vortex Flow in Nature and Technology*; Wiley-Interscience: New York, 1983.
40. Robinson, S.K. Coherent motions in the turbulent boundary layer. *Annual Review of Fluid Mechanics* **1991**, *23*(1), 601–639.
41. Jiang, M.; Machiraju, R.; Thompson, D. *Detection and visualization of. In The Visualization Handbook*; Hansen, C.D., Ohnson, C.R., Eds.; Elsevier: New York, 2005; 295.
42. Keshani, S.; Daud, W.R.W.; Woo, M.W.; Nourouzi, M.; Talib, M.Z.M.; Chuah, A.L.; Russly, A. Evaluation of drying conditions on full cream milk produced by nitro-spray dryer. Presented at the 5th Asian Particle Technology Symposium; Singapore, July 2–5, 2012.
43. Keshani, S.; Daud, W.R.W.; Woo, M.W.; Nourouzi, M.; Talib, M.Z.M.; Chuah, A.L.; Russly, A. Reducing the deposition of fat and protein covered particles with low energy surfaces. *Journal of Food Engineering* **2013**, *116*(3), 737–748.